

Targeted Delivery of Exosome-Derived miRNA-185-5p Inhibitor via Liposomes Alleviates Apoptosis and Cuproptosis in Dilated Cardiomyopathy

Shuai Xu^{1-5,*}, Yiyao Zeng^{1,2,*}, Xin Tan^{1,2}, Ge Zhang³⁻⁵, Anchen Xu^{1,2}, Huimin Fan⁶, Fengyi Yu⁷, Zhen Qin³⁻⁵, Yahui Song⁶, Yufeng Jiang^{1,2}, Xiangyu Wang^{1,2}, Duoduo Zhang⁸, Yuxin Nong^{1,2}, Dede Lian⁹, Junnan Tang³⁻⁵, Yafeng Zhou^{1,2}

¹Department of Cardiology, The Fourth Affiliated Hospital of Soochow University, Suzhou Dushu Lake Hospital, Medical Center of Soochow University, Suzhou, 215000, People's Republic of China; ²Institute for Hypertension, Soochow University, Suzhou, 215000, People's Republic of China; ³Department of Cardiology, The First Affiliated Hospital of Zhengzhou University, Zhengzhou, 450052, People's Republic of China; ⁴Department of Cardiology, Henan Province Key Laboratory of Cardiac Injury and Repair, Zhengzhou, 450052, People's Republic of China; ⁵Department of Cardiology, Henan Province Clinical Research Center for Cardiovascular Diseases, Zhengzhou, 450052, People's Republic of China; ⁶Center of Translational Medicine and Clinical Laboratory, The Fourth Affiliated Hospital to Soochow University, Suzhou, 215028, People's Republic of China; ⁷College of Veterinary Medicine, NC State University, Raleigh, NC, USA; ⁸Department of Thoracic Surgery, The First Hospital of Jilin University, Changchun, 130021, People's Republic of China; ⁹Department of Intensive Care Medicine, China-Japan Union Hospital of Jilin University, Changchun, 130033, People's Republic of China

*These authors contributed equally to this work

Correspondence: Yafeng Zhou, Department of Cardiology, The Fourth Affiliated Hospital of Soochow University, Suzhou Dushu Lake Hospital, Medical Center of Soochow University, Suzhou, 215000, People's Republic of China, Email Dryafengzhou@163.com; Junnan Tang, Department of Cardiology, The First Affiliated Hospital of Zhengzhou University, Zhengzhou, Henan, 450052, People's Republic of China, Email fcctangjn@zzu.edu.cn

Purpose: Dilated cardiomyopathy (DCM) is a prevalent form of heart failure with limited therapeutic options. This study explores a novel treatment strategy involving the delivery of exosome-derived miRNA-185-5p inhibitors encapsulated in liposomes, aiming to target cardiac tissue and alleviate myocardial apoptosis and cuproptosis in DCM.

Methods: The miRNA-185-5p inhibitor, identified in our previous study and extracted from exosomes, was encapsulated in liposomes functionalized with a cardiac-targeting peptide. This system was used in both in vitro and in vivo models of DCM induced by doxorubicin (DOX). We evaluated the effects of this treatment on cardiac function, apoptosis, cuproptosis, oxidative stress, and fibrosis using echocardiography, histological analysis, Western blotting, and biochemical assays.

Results: In vitro experiments demonstrated that the Lipo@miR-185-5p inhibitor markedly attenuated apoptosis and cuproptosis in H9C2 cells and iPSC-derived cardiomyocytes, with a 42.6% reduction in apoptotic cell rates and over 50% downregulation of cuproptosis-related markers (both $P < 0.01$). In vivo, the targeted liposomal formulation significantly improved cardiac function in DOX-induced DCM mice, as evidenced by a 27.3% increase in left ventricular ejection fraction (LVEF) and a 36.5% reduction in myocardial fibrosis area ($P < 0.01$), along with enhanced survival. These findings underscore the therapeutic potential of this targeted delivery strategy for the treatment of dilated cardiomyopathy.

Conclusion: Lipo@miR-185-5p inhibitor, utilizing exosome-derived miRNA and targeted liposomal delivery, effectively alleviates DCM-induced myocardial dysfunction. This approach represents a promising therapeutic strategy for cardiovascular diseases by targeting specific molecular mechanisms involved in heart failure.

Keywords: liposome, exosome-miR-185-5p inhibitor, dilated cardiomyopathy, apoptosis, cuproptosis

Introduction

Dilated cardiomyopathy (DCM) is a prevalent form of heart failure, characterized by left ventricular (LV) dilation and systolic dysfunction in the absence of abnormal loading conditions, such as hypertension or severe coronary artery

disease.¹ The condition is associated with high morbidity and mortality, and is a major cause of sudden cardiac arrest and heart transplantation.^{2,3} The etiology of DCM is multifactorial, involving genetic factors, viral infections, and exposure to toxins. Despite advances in imaging, genetic analysis, and biopsy techniques, up to 50% of DCM patients still present with an unidentified etiology.⁴ Current therapeutic approaches primarily address symptom management, reduction of sudden cardiac death risk, attenuation of disease progression, and prevention of systemic complications. Nevertheless, despite progress in pharmacological and interventional therapies, the prognosis for patients with DCM remains unfavorable, largely due to the absence of targeted treatments addressing the root cause of the disease.⁵

Conventional treatments—ACE inhibitors, beta-blockers, diuretics, ARNIs, and SGLT2 inhibitors—provide limited survival benefit, and device-based interventions like ICDs and CRT are primarily supportive.^{6,7} While these therapies alleviate symptoms, they fail to prevent disease progression or address the molecular drivers of DCM.

Given these limitations, there is increasing recognition of the urgent need for innovative therapeutic strategies capable of halting or reversing the progression of DCM. Targeted molecular therapies, including gene therapy, miRNA modulation, and advanced drug delivery systems, offer promising alternatives by addressing the underlying pathophysiological mechanisms of the disease.⁸ Emerging studies have identified mutations in genes encoding sarcomeric, cytoskeletal, and mitochondrial proteins, contributing to the structural and functional deterioration characteristic of DCM.⁹

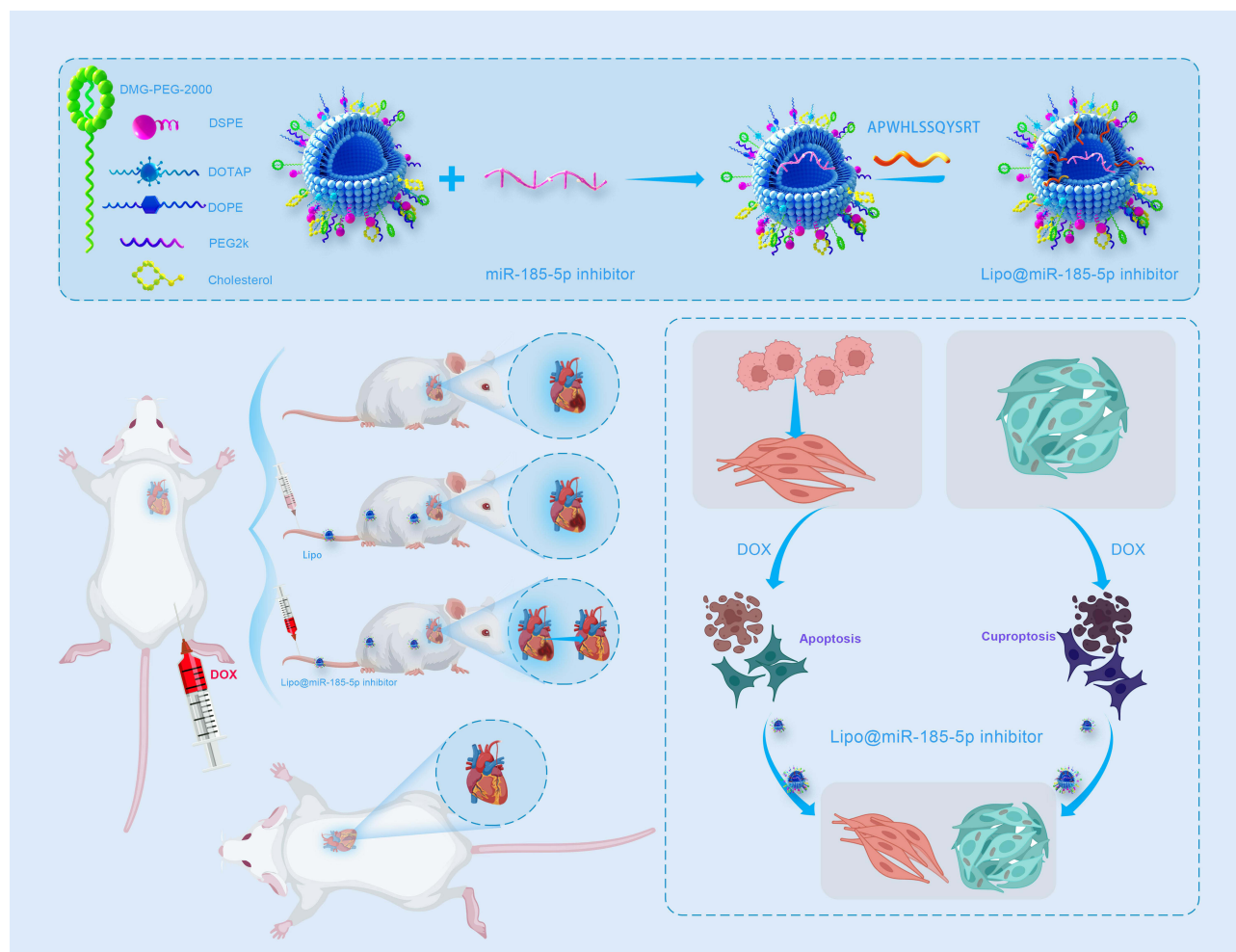
Our previous studies have revealed that elevated expression of miR-185-5p plays a crucial role in promoting collagen production and triggering pro-fibrotic activation in fibroblasts.¹⁰ Inhibition of miR-185-5p, on the other hand, has been shown to significantly reduce collagen synthesis. Analysis of ventricular tissues from severe cardiomyopathy patients revealed that miR-185-5p expression correlates with increased TGF- β 1 and collagen I levels.¹¹ Further studies have shown that miR-185-5p promotes mitochondrial dysfunction and cardiac hypertrophy, reinforcing its key role in DCM pathogenesis.¹²

In recent years, nanomaterials have been extensively investigated within the medical field due to their unique physicochemical properties and superior biocompatibility.¹³ Among nanomaterials, liposomes are favored for their biocompatibility and ability to encapsulate diverse drugs for targeted delivery. Several liposome-based nanomedicines, such as Onivyde, Marqibo, Doxil, Visudyne, and DepoCyt, have received approval from the US Food and Drug Administration (FDA) for clinical use in cancer therapy.¹⁴ By enhancing the bioavailability of encapsulated therapeutics, liposomes significantly improve treatment efficacy while minimizing systemic side effects.¹⁵

A key advantage of liposomes is their ability to be functionalized with targeting ligands, enabling receptor-mediated delivery and selective accumulation in diseased tissues. This targeted approach enhances therapeutic efficacy while reducing off-target effects.¹⁶ For example, peptide-functionalized liposomes have been shown to substantially enhance the delivery of chemotherapeutic agents to tumors, improving therapeutic outcomes while mitigating toxicity.¹⁷ Liposomes also provide an effective platform for delivering gene therapies such as miRNA inhibitors, protecting them from degradation and enhancing cellular uptake. When targeted to cardiac tissue, miRNA-loaded liposomes can down-regulate pathogenic miRNAs and improve cardiac function.¹⁸

Apoptosis is one of the key mechanisms of cardiomyocyte death in patients with DCM, with research indicating a strong correlation between cardiomyocyte apoptosis, ventricular remodeling, and functional impairment.¹⁹ Moreover, cuproptosis, a newly recognized form of programmed cell death, has garnered increasing attention for its role in cardiovascular diseases.²⁰ Studies have shown that copper overload induces intracellular oxidative stress and mitochondrial dysfunction, leading to cardiomyocyte injury and death.²¹ Although not fully defined in DCM, copper-induced mitochondrial dysfunction and oxidative stress are implicated in cardiomyocyte damage. Notably, the interplay between apoptosis and other regulated cell death pathways, such as cuproptosis, may significantly influence the progression of DCM.²² These findings highlight the therapeutic potential of simultaneously targeting apoptosis and cuproptosis to preserve cardiomyocytes and improve cardiac function in DCM. Further research into these mechanisms is crucial for the development of more effective therapies.

In this study, we explored the encapsulation of exosome-miRNA-185-5p inhibitors within liposomes conjugated with targeting peptides (Lipo@miR-185-5p inhibitor), designed to enhance their delivery to cardiac tissue (Scheme 1). This miRNA was selected based on its critical role in DCM pathophysiology, extending our previous research.¹⁰ By inhibiting pathogenic miRNAs, this strategy aims to reduce apoptosis and inflammation, thereby improving cardiac function. The combination of exosomes and liposomes enhances both the biocompatibility and targeted delivery of miRNA inhibitors,



Scheme 1 Schematic representation of the preparation and cardiac-targeted delivery of Lipo@miR-185-5p inhibitor, including tail vein administration in DCM mice and subsequent validation of therapeutic effects through in vitro cardiomyocyte assays.

with exosomes providing natural cellular uptake mechanisms and liposomes ensuring the stability and precise delivery of the therapeutic agents. Through comprehensive in vitro and in vivo experimentation, this research aims to establish a targeted miRNA inhibitor therapy for DCM, with the overarching objective of improving clinical outcomes and enhancing patient quality of life.

Materials and Methods

Materials

Polycarbonate membranes were purchased from Whatman (UK). 1,2-Dioleoyl-3-trimethylammonium-propane (DOTAP), 1,2-Dioleoyl-sn-glycero-3-phosphoethanolamine (DOPE), cholesterol, 1,2-Dioleoyl-sn-glycero-3-phosphoethanolamine-N-[methoxy(polyethyleneglycol)-2000] (DMG-PEG-2000), 1,2-Distearoyl-sn-glycero-3-phosphoethanolamine (DSPE), polyethylene glycol-2000 (PEG2k), and the targeting peptide APWHLSSQYSRT were all obtained from Xi'an Ruixi Biological Technology Co., Ltd. Cell counting kit-8 (CCK-8) was obtained from Djourdi Laboratories (Kumamoto, Japan). The assay kits for total cholesterol (TC), alanine aminotransferase (ALT), aspartate aminotransferase (AST), albumin (ALB), blood urea nitrogen (BUN), and creatinine (CRE) were purchased from Beyotime Biotechnology (Beyotime, China).

Lipo@miR-185-5p Inhibitor Preparation

To prepare Lipo@miR-185-5p inhibitor, DOTAP, DOPE, cholesterol, DMG-PEG-2000, and DSPE-PEG2k-APWHLSSQYSRT were dissolved in chloroform. A thin lipid film was formed through rotary evaporation under reduced pressure, followed by drying to ensure complete solvent removal. After drying, 4 mL of deionized water was added for hydration. The resulting dispersion was extruded through a polycarbonate membrane with a pore size of 100 nm using a liposome extruder to achieve uniform liposome formation. Subsequently, the liposomes were dialyzed against deionized water using a polycarbonate membrane nanopore dialysis device with a pore size of 10 nm to remove unencapsulated components. The final volume of the liposome suspension was adjusted to 5 mL with deionized water. Following dialysis, the liposome suspension was sterilized by incubation at 70°C for 3 hours. Under sterile conditions, the miR-185-5p inhibitor, previously dissolved in diethyl pyrocarbonate (DEPC)-treated water, was incorporated into the liposomes through passive loading, with thorough mixing achieved by repeated pipetting. A lyoprotectant was added to the solution to preserve the liposomes during storage, followed by lyophilization to obtain stable RNA-loaded liposomes for subsequent applications.

Characterization of Lipo@miR-185-5p Inhibitor

Following negative staining, the morphology of the liposomes and Lipo@miR-185-5p inhibitor was observed using transmission electron microscopy (TEM) (FEI, USA). The hydrodynamic diameter and zeta potential of the liposomes and Lipo@miR-185-5p inhibitor were measured in PBS using the NanoBrook 90plus PALS particle size analyzer (Brookhaven Instruments, USA).

Encapsulation and Releasing Capacity of Lipo@miR-185-5p Inhibitor

The encapsulation efficiency and release profile of Lipo@miR-185-5p inhibitor were evaluated using UV-Visible spectroscopy. The absorption peak of miR-185-5p inhibitor was utilized for quantitative analysis. To construct Lipo@miR-185-5p inhibitor, miRNA inhibitor and lipids (DOTAP, DOPE, cholesterol, and DMG-PEG2k-APWHLSSQYSRT) were mixed at a mass ratio of 29:4:8:1. After ultrafiltration, Lipo@miR-185-5p inhibitor was resuspended in an equal volume of PBS, followed by the addition of an equal volume of absolute ethanol, and sonicated in a water bath. The absorbance of the miRNA inhibitor was subsequently measured, with blank liposomes undergoing the same process to ensure that their absorbance was subtracted for accurate analysis. For the *in vitro* drug release assay, the concentration of Lipo@miR-185-5p inhibitor was determined using high-performance liquid chromatography (HPLC). Liposome dispersions from dialysis bags were collected at predetermined time points (0h, 1h, 2h, 4h, 8h, 24h, and 48h). The liposome structure was disrupted using Triton extraction to release the encapsulated Lipo@miR-185-5p inhibitor. The aqueous phase was collected, and absorbance was measured using HPLC at the maximum absorption wavelength. The cumulative release profile was obtained by determining the concentration of Lipo@miR-185-5p inhibitor at various time points, with the maximum absorption wavelength around 340 nm.

Cell Lines and Cell Culture

The rat cardiomyocyte cell line H9C2 was purchased from BeNa Culture Collection (BNCC, China). The cells were cultured in Dulbecco's modified Eagle medium (DMEM; Gibco, USA) supplemented with 10% fetal bovine serum (FBS) and antibiotics (100 units of penicillin and 100 µg of streptomycin per milliliter; Gibco, USA). The cells were maintained at 37°C in a humidified atmosphere with 5% CO₂. The culture medium was replaced every 2–3 days, and the cells were passaged when they reached 70–80% confluence. Cells were seeded at the appropriate density according to the experimental design. Normal human cord blood cell-derived iPSC lines were obtained from Meisen CTCC (China). The hiPSCs were cultured in TeSR-E8 medium (Stemcell Technologies, Vancouver, BC, Canada) on vitronectin-coated plates and passaged every four days using the ReLeSR reagent (Stemcell Technologies). The differentiation of hiPSCs into cardiomyocytes followed a previously established protocol. Specifically, the cells were seeded onto Matrigel-coated six-well plates and, upon reaching approximately 90% confluence, were incubated in RPMI 1640 medium supplemented with B27 (without insulin) and 10µM CHIR99021 (MCE) to activate Wnt signaling and induce mesoderm

differentiation. After three days, the medium was replaced with RPMI 1640 + B27 (without insulin) and supplemented with C59 (Prunoyce) to continue the differentiation process. After 48 hours, the medium was changed to RPMI 1640 + B27 without insulin or RPMI 1640 + B27 with insulin. The cells were then metabolically purified from other differentiated cell types by glucose deprivation, using RPMI 1640 without glucose and B27 with insulin, as described in previous protocols. In this study, H9C2 cells and iPSC-derived cardiomyocytes were exposed to 2 μ M doxorubicin (DOX; MCE) for 24 hours to simulate an *in vitro* model of dilated cardiomyopathy. DOX was prepared as a 2 mM stock solution in sterile DMSO and diluted to the working concentration in culture medium. After 24 hours of DOX exposure, the cells were washed with PBS and fresh medium was added for subsequent analysis. The successful induction of the DCM model was confirmed by a reduction in cell viability and an increase in apoptotic activity, consistent with the established characteristics of DCM.

Optimization of Lipo@miR-185-5p Inhibitor Concentration Using CCK8 Assay

To determine the optimal therapeutic concentration of the Lipo@miR-185-5p inhibitor in DOX-induced H9C2 and iPSC-derived cardiomyocytes, cell viability was assessed using the CCK8 assay. DOX-induced H9C2 cells and iPSC-derived cardiomyocytes were treated with varying concentrations of Lipo@miR-185-5p inhibitor (0, 3.75, 6.75, 10, 15, and 20 μ M) in triplicate. After 24 hours of treatment, 10 μ L of CCK8 reagent (Dojindo, Japan) was added to each well, and the plates were incubated at 37°C for 2 hours. Absorbance was measured at 450 nm using a microplate reader. A dose-response curve was generated from the cell viability data, and the optimal concentration of Lipo@miR-185-5p inhibitor was determined for subsequent validation in the DOX-induced DCM model.

Doxorubicin-Induced Cardiotoxicity Animal Model

C57BL/6 male mice (weighing 20–30 g, SPF grade, certification number 202408A0374) were obtained from the Experimental Animal Center of Soochow University, China. All animal experiments were approved by the Ethics Committee of Soochow University and conducted in accordance with the Guide for the Care and Use of Laboratory Animals (NIH Publication No. 85–23, revised 1996). The mice were randomly assigned to four experimental groups: the normal control group, the Dox group, the empty liposome combined with Dox group, and the Lipo@miR-185-5p combined with Dox group. Doxorubicin (Dox) was administered intraperitoneally in four equal doses over 3 weeks, with a cumulative dose of 300 mg/kg. The injection dose of Lipo@miR-185-5p inhibitor was selected based on preliminary dose-response studies and previous reports of miRNA delivery in cardiac disease models. A dose of 5 mg/kg (corresponding to 0.1 mg per mouse, dissolved in 100 μ L ultrapure water) was administered via tail vein injection. This dose was confirmed to achieve effective therapeutic responses while minimizing off-target toxicity. The liposomes and Lipo@miR-185-5p inhibitor were injected every 2 to 3 days over a period of 2 to 4 weeks. To assess therapeutic efficacy, echocardiography and serum myocardial injury biomarkers were measured. At the end of the experiment, histological analysis was conducted, and liver, lung and kidney function were monitored to evaluate systemic toxicity of the treatment.

Biodistribution of Liposome@CY5.5-Encapsulated miR-185-5p Inhibitor by *in vivo* Imaging System

To evaluate the heart-targeting efficiency of liposomes encapsulating miR-185-5p inhibitor with a targeting peptide, Liposome@CY5.5-miR-185-5p inhibitor was prepared with an approximate particle size of 100 nm. Male C57BL/6 mice (weighing 20–30g) were used to establish a doxorubicin (DOX)-induced dilated cardiomyopathy (DCM) model. After 10 days of acclimatization, the mice were randomly assigned to two groups: one group received liposomes containing the targeting peptide (Lipo-HT), while the other group received liposomes without the targeting peptide (Lipo-V).

Both groups were intravenously injected with 100 μ L of Liposome@CY5.5-miR-185-5p inhibitor via the tail vein, corresponding to a dose of approximately 5 mg/kg per injection. To monitor the biodistribution of the liposomes and assess heart-specific targeting, *in vivo* imaging was performed at predetermined time points (2, 8, 12, and 24 hours) using an *in vivo* imaging system (IVIS Spectrum, USA). Following the final imaging time point, the mice were euthanized, and

major organs (heart, lungs, spleen, liver, and kidneys) were harvested. Fluorescence signals from these tissues were captured and analyzed to evaluate the accumulation of liposomes in the heart compared to other organs. This allowed for an assessment of the targeting efficiency of Lipo@miR-185-5p inhibitor with the targeting peptide, in comparison to the non-targeted liposomes.

Echocardiography and Histological Analysis

Three weeks after Dox stimulation, left ventricular function in the mice was assessed using echocardiography. Mice were randomly divided into four groups: Control (CON), DOX, DOX with Empty Liposome (Lipo), and DOX with Targeted Lipo@miR-185-5p inhibitor (Lipo@miR-185-5p group). A two-dimensional M-mode echocardiography technique was employed, utilizing the Technos MPX ultrasound system (ESAOTE, Italy). Key cardiac function parameters measured included ejection fraction (EF), fractional shortening (FS), left ventricular anterior wall thickness at end-diastole (LVAW;d), left ventricular anterior wall thickness at end-systole (LVAW;s), left ventricular posterior wall thickness at end-diastole (LVPW;d), left ventricular posterior wall thickness at end-systole (LVPW;s), left ventricular internal diameter at end-diastole (LVID;d), left ventricular internal diameter at end-systole (LVID;s), and cardiac output (CO).

Upon completion of the echocardiographic assessment, the mice were euthanized via cervical dislocation. Immediately following euthanasia, the abdominal and thoracic cavities were opened, and major organs, including the heart, liver, kidneys, and lungs, were harvested. The tissues were washed three times with cold PBS to remove blood and other contaminants. The organs were then sectioned into appropriately sized blocks along anatomical planes and fixed in 4% paraformaldehyde for 24 hours to preserve tissue architecture.

Following fixation, all tissue samples underwent standard procedures for dehydration and paraffin embedding. Histological staining was carried out by Servicebio (Wuhan, China). Hematoxylin-eosin (HE) staining was employed to observe the overall morphological characteristics of the heart, liver, kidney, and lung tissues, specifically assessing for signs of inflammation, necrosis, fibrosis, or other potential toxicological responses. For cardiac tissue, Masson's trichrome staining was performed to evaluate the extent of myocardial fibrosis, particularly focusing on collagen fiber deposition. All stained tissue sections were examined using microscopy, and quantitative analysis of the images was conducted with ImageJ software to compare histological changes and assess potential systemic toxic effects across the different treatment groups.

Detection of Biochemical Markers of Myocardial Injury

To evaluate the therapeutic effects of Lipo@miR-185-5p inhibitor on doxorubicin (Dox)-induced myocardial injury, biochemical markers of cardiac damage were analyzed in mouse serum. The myocardial injury markers included cardiac troponin I (cTnI), creatine kinase-MB (CK-MB), lactate dehydrogenase (LDH), and NT-proBNP. At the conclusion of the experiment, the mice were euthanized by cervical dislocation, and blood samples were collected through cardiac puncture. After allowing the samples to sit at room temperature for 30 minutes, serum was obtained by centrifugation at 3000 rpm for 10 minutes at 4°C, and the separated serum samples were stored at -80°C for later analysis.

The concentrations of cTnI, CK-MB, and NT-proBNP in the serum were measured using ELISA kits (from Abcam and Thermo Fisher), following the manufacturer's protocols. Initially, diluted serum samples were added to a 96-well plate, followed by incubation and washing. Subsequently, enzyme-labeled antibodies were introduced, and unbound materials were removed through additional incubation and washing steps. A colorimetric substrate was added to facilitate the color reaction, and absorbance was measured at 450 nm using a microplate reader. The concentrations of the biochemical markers were determined by constructing standard curves. By comparing the levels of these biochemical markers among different experimental groups (Control Group, DOX Group, Empty liposome+DOX group, and Lipo@miR-185-5p+DOX group), the protective effects of Lipo@miR-185-5p against DOX-induced myocardial injury were assessed.

Western Blot Analysis

After differentiating induced pluripotent stem cells (iPSCs) into cardiomyocytes, cells were divided into four experimental groups: Control Group, DOX Group, Empty Liposome+DOX group, and Lipo@miR-185-5p+DOX group. Total cellular proteins were extracted using RIPA lysis buffer containing a protease inhibitor cocktail. The protein

concentrations were quantified using the BCA method, and equal amounts of protein from each group were loaded onto a polyacrylamide gel for separation by sodium dodecyl sulfate-polyacrylamide gel electrophoresis (SDS-PAGE). Following SDS-PAGE, the separated proteins were transferred to nitrocellulose (NC) membranes. The membranes were then blocked with a rapid blocking solution to prevent non-specific binding. Subsequently, the membranes were incubated overnight at 4°C with primary antibodies against Bcl-2, Bax, Caspase-3, Cleaved Caspase-3, DLAT, DLST, FDX1, and the loading control β -actin. After primary antibody incubation, the membranes were incubated with HRP-conjugated secondary antibodies at room temperature for 1 hour.

Protein expression was visualized using the BIO-RAD ChemiDoc XRS chemiluminescence system (Bio-Rad Laboratories, CA, USA). The intensity of the protein bands was quantified using ImageJ software, and the protein expression levels were normalized to β -actin as an internal control. This normalization allowed for a comparative analysis of the expression levels of apoptosis- and cuproptosis-related proteins across the experimental groups.

Immunofluorescence Staining

To establish an *in vitro* model of doxorubicin (DOX)-induced dilated cardiomyopathy (DCM), H9C2 cells were treated with DOX and divided into three experimental groups: Control Group, DOX Group, and Lipo@miR-185-5p + DOX Group. Immunofluorescence staining was performed to assess levels of apoptosis, DNA damage, and oxidative stress using specific probes: TUNEL (for apoptosis), γ H2AX (for DNA damage), and ROS (for oxidative stress). After treatment, the H9C2 cells were fixed on culture plates with 4% paraformaldehyde, washed three times with PBS (5 minutes per wash), and permeabilized with 0.1% Triton X-100. A 30-minute blocking step was performed to prevent non-specific binding. Subsequently, the cells were incubated with TUNEL reagent, γ H2AX primary antibody, and the ROS probe, following the manufacturer's instructions for the appropriate incubation times and conditions. After incubation, the cells were washed three times with PBS (5 minutes per wash), and fluorescence images were captured using a fluorescence microscope. Fluorescence intensity in each group was quantified using ImageJ software to assess differences in apoptosis, DNA damage, and ROS levels. These analyses provided insight into the degree of cell injury and repair under different treatment conditions, allowing for a comparative evaluation of the therapeutic effects of Lipo@miR-185-5p against DOX-induced damage.

Myocardial Copper Quantification

Myocardial copper levels were measured using a Cu^{2+} colorimetric assay kit (Chelation Method; Elabscience, China) according to the manufacturer's protocol. Briefly, fresh heart tissues were homogenized in extraction buffer, and the supernatants were collected after centrifugation. Absorbance was measured at 580 nm using a microplate reader. Copper concentrations were calculated based on a standard curve (detection range: 1.84–60 $\mu\text{mol/L}$; sensitivity: 1.84 $\mu\text{mol/L}$). All measurements were performed in triplicate.

Statistical Analysis

All experimental data are presented as mean \pm standard deviation (SD) and were analyzed using SPSS software. Statistical significance was determined using an independent *t*-test or one-way ANOVA, as appropriate.

Result and Discussion

Physicochemical Characterization of the Lipo@miR-185-5p Inhibitor Complex

The Lipo@miR-185-5p inhibitor was synthesized using the lipid film hydration method followed by membrane extrusion (Scheme 1). This method reliably produces liposomes with uniform particle sizes and stable morphologies, which are crucial for drug delivery applications. TEM images revealed smooth, spherical liposomal nanoparticles with an average diameter of approximately 100 nm, with no observable differences between the blank liposomes and the miRNA-loaded liposomes (Figure 1A and B). These findings suggest that the encapsulation process preserves the structural integrity of the liposomes, consistent with previous studies on lipid-based miRNA carriers. Such structural stability ensures uniform biodistribution and controlled drug release, making the formulation suitable for therapeutic delivery.

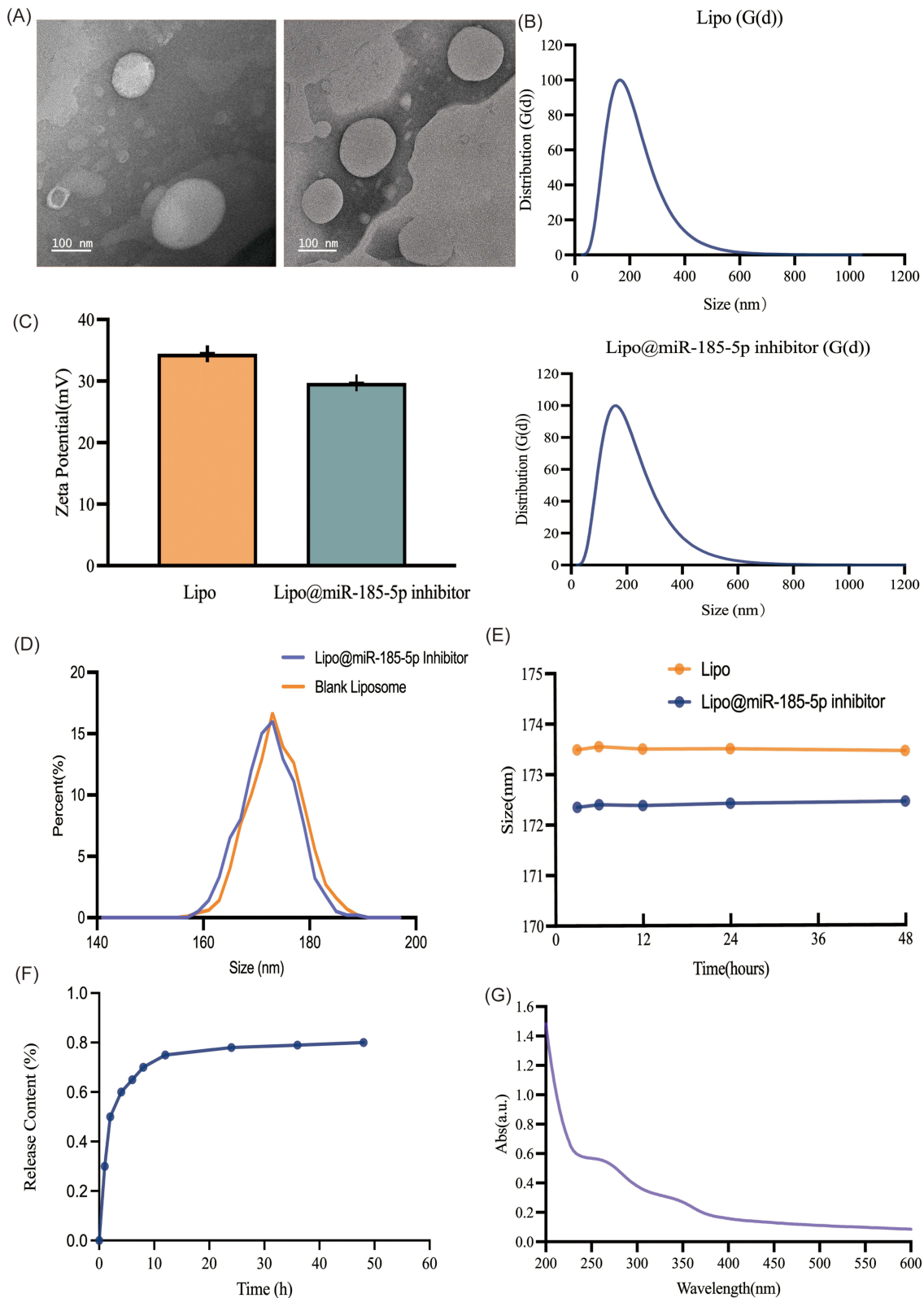


Figure 1 Characterization of Lipo@miR-185-5p inhibitor: **(A)** Representative TEM images of Liposome and Lipo@miR-185-5p inhibitor, scale bar = 100 nm. **(B)** Particle size distribution of Liposome and Lipo@miR-185-5p inhibitor from TEM observation. **(C)** Zeta potential measurements showing surface charges of blank liposomes (34.4 mV) and Lipo@miR-185-5p inhibitor (29.7 mV), indicating successful miRNA encapsulation. **(D)** Hydrodynamic size of Liposome and Lipo@miR-185-5p inhibitor in PBS. **(E)** Average hydrodynamic size of Liposome and Lipo@miR-185-5p inhibitor at various time points (0, 3, 6, 12, 24, 48 hours) in PBS. **(F)** In vitro release profile of Lipo@miR-185-5p inhibitor in pH 7.4 PBS at room temperature over 48 hours. **(G)** UV-visible absorption spectrum of Lipo@miR-185-5p inhibitor. The characteristic absorbance peak of miR-185-5p inhibitor is indicated at 350 nm. (EE% = 98.0 ± 1.2%).

Zeta potential analysis indicated that the cationic blank liposomes and Lipo@miR-185-5p inhibitor exhibited surface charges of 34.4 mV and 29.7 mV, respectively (Figure 1C). The positive zeta potential of cationic liposomes facilitates efficient interaction with negatively charged cell membranes, enhancing cellular uptake. The slight reduction in zeta potential upon miRNA encapsulation is attributed to partial neutralization of the surface charge by the negatively charged miRNA molecules. This observation aligns with previous reports on miRNA-loaded liposomes, which similarly demonstrated minor reductions in zeta potential upon payload incorporation.¹⁸

Dynamic light scattering (DLS) measurements revealed a minor change in the hydrodynamic diameter of liposomes following encapsulation. DLS analysis indicated that the average hydrodynamic diameter decreased slightly from 173.49 ± 0.9 nm for blank liposomes to 172.35 ± 0.8 nm for Lipo@miR-185-5p inhibitor, with polydispersity indices (PDI) less than 0.15, confirming a narrow size distribution (Figure 1D). This reduction in size is consistent with previous findings, where the incorporation of negatively charged miRNA resulted in a reduction of electrostatic repulsion between liposomes, leading to a more compact structure.¹⁸ Additionally, changes in the hydrated shell thickness or the reorganization of the lipid bilayer upon miRNA encapsulation may further explain the observed size reduction. This minor change suggests successful miRNA encapsulation without altering the overall stability or functionality of the liposomes.

The hydrodynamic diameters of both blank liposomes and Lipo@miR-185-5p inhibitor remained stable over 48 hours in PBS, with no significant change observed (Figure 1E), indicating good colloidal stability. Stability in physiological solutions is a critical parameter, as it predicts the shelf life and effectiveness of the delivery system in biological environments. Previous studies have demonstrated that cationic liposomes exhibit good stability in PBS due to electrostatic repulsion between particles, preventing aggregation.²³ The stability observed in this study is consistent with these findings, reinforcing the potential of Lipo@miR-185-5p inhibitor as a robust delivery vehicle.

The *in vitro* drug release profile of Lipo@miR-185-5p inhibitor in pH 7.4 PBS at room temperature over 48 hours demonstrated a biphasic release pattern. A rapid release phase occurred within the first 8 hours, followed by a sustained release that plateaued at 80% (Figure 1F). This controlled release behavior ensures both immediate and prolonged therapeutic effects, supporting the potential of this delivery system for miRNA-based applications.

To evaluate the encapsulation efficiency of the cationic liposomes, Lipo@miR-185-5p inhibitor (approximately 100 nm in size) was prepared using different mass ratios of miR-185-5p inhibitor to cationic liposomes, resulting in an encapsulation efficiency of $98\% \pm 1.2\%$. This high encapsulation efficiency is favorable for therapeutic applications, as it ensures a substantial payload is delivered to target sites, maximizing therapeutic efficacy. The high efficiency observed here can be attributed to the strong electrostatic interactions between the cationic liposomes and the negatively charged miR-185-5p molecules, consistent with previous reports on miRNA encapsulation using cationic carriers.²⁴ UV-visible spectrophotometry confirmed the successful encapsulation of miR-185-5p inhibitor, as evidenced by a characteristic absorption peak near 350 nm (Figure 1G). This absorption feature reflects the presence of miRNA and has been widely adopted as a non-invasive technique to assess loading efficiency in RNA-loaded nanoparticles. The reproducibility and robustness of this spectral method further support its reliability for miRNA quantification in liposomal formulations.

Overall, these findings demonstrate that the Lipo@miR-185-5p inhibitor complex maintains stability, exhibits favorable size and charge characteristics, and achieves a high encapsulation efficiency, supporting its suitability as an effective delivery vehicle for miRNA-based therapies. Compared to previous studies, this formulation achieves similar or improved performance metrics, particularly in terms of stability and encapsulation efficiency, further reinforcing the potential of cationic liposome carriers in targeted miRNA delivery systems for therapeutic applications.²⁵

Evaluation of Significant Accumulation and Distribution of Heart-Targeted Liposomes in the Heart Following Tail Vein Injection

To investigate the tissue distribution of liposomes encapsulating miRNA 185–5p inhibitor, modified with the heart-targeting peptide APWHLSSQYSRT, in a dilated cardiomyopathy (DCM) mouse model, liposomes were labeled with the near-infrared fluorescent dye CY5.5. This dye, known for its deep tissue penetration and low autofluorescence, allows precise tracking of liposome distribution *in vivo*. After encapsulating CY5.5, the liposome size slightly increased, with a hydrodynamic diameter

of approximately 183.50 nm, demonstrating good stability (Figure S1). Such minor increases are consistent with prior studies, suggesting successful incorporation of CY5.5 into the lipid bilayer without compromising structural integrity.²⁶

Fluorescence imaging revealed significantly stronger Cy5.5 signal accumulation in the heart tissue of the Lipo-HT group at all time points, particularly at 8 and 12 hours post-injection, indicating enhanced cardiac targeting conferred by the peptide modification. In contrast, the Lipo-V group exhibited a more dispersed distribution, with prominent signals in the liver and spleen but relatively weak cardiac accumulation. Quantitative analysis confirmed that the fluorescence intensity in the heart was significantly higher in the Lipo-HT group compared to the Lipo-V group ($P < 0.01$), confirming the effectiveness of the targeting strategy. In comparison, the liposomes with the targeting peptide showed significant accumulation in heart tissue at different time points, while their distribution in other organs, such as the liver and spleen, markedly decreased over time, indicating that the targeting peptide successfully directed the liposomes to preferentially concentrate in the heart (Figure 2A). This finding is consistent with previous studies that demonstrated the use of organ-specific targeting peptides could significantly improve the localization of therapeutic agents to designated organs, enhancing therapeutic outcomes while minimizing off-target effects. Recent advancements in targeted delivery systems have significantly enhanced the therapeutic efficacy of treatments for cardiovascular diseases.²⁷ In particular, the use of heart-targeting peptides has shown promise in directing therapeutic agents specifically to cardiac tissues, thereby improving treatment outcomes and reducing off-target effects. For instance, Li et al²⁸ developed liposomes encapsulating microRNA-21 (miR-21) mimics, modified with a cardiac troponin T (cTnT) antibody for targeted delivery to ischemic myocardium. The targeted liposomes exhibited enhanced accumulation in ischemic heart tissue, leading to improved cardiac function and reduced infarct size in a rat model of acute myocardial infarction.

Further histological analysis was conducted to evaluate the safety of the liposomes on major organs using hematoxylin and eosin (HE) staining. At the end of the experiment, liver, lung, and kidney tissues were collected and stained with HE. The results showed no significant inflammation, tissue damage, or other pathological changes in the Lipo-HT groups compared to the control group, indicating no evident toxicity of the liposomes on major organs (Figure 2B). These findings are supported by previous research suggesting that lipid-based nanoparticles, due to their biocompatibility, often exhibit minimal toxicity, making them suitable for long-term therapeutic applications.²⁹ Serum biochemical analysis at 24 hours post-injection revealed no significant differences in CRE, BUN, ALT, AST, Alb, and TC levels among groups (Figure 2C), indicating favorable biocompatibility and no detectable off-target toxicity associated with Lipo@miR-185-5p inhibitor administration. This safety profile aligns with previous studies where lipid-based carriers exhibited negligible systemic toxicity, highlighting their potential for repeated administrations in chronic conditions.³⁰

In summary, tail vein injection of liposomes modified with a heart-targeting peptide significantly enhanced their accumulation in cardiac tissue while reducing distribution in other major organs, without inducing organ toxicity or damage. This underscores the strong cardiac-targeting efficiency and safety of the modified liposomes. In this study, liposomes in the Lipo@miR-185-5p group exhibited substantial accumulation in heart tissue, whereas liposomes in the empty Lipo group primarily accumulated in organs such as the liver and spleen. This indicates that the addition of the cardiac-targeting peptide markedly improved the targeting efficiency of liposome delivery to the heart. This enhanced targeting aligns with findings from recent studies employing similar targeting peptides, which reported increased tissue accumulation through peptide-mediated receptor binding, thereby confirming the efficacy of organ-specific peptide targeting strategies.³¹

Additionally, serum biochemical analysis revealed no significant toxicity to liver or kidney function in the Lipo@miR-185-5p inhibitor group, further confirming its *in vivo* safety. The absence of toxic effects on the liver and kidneys underscores the strong potential for clinical application of this formulation, making it especially suitable for patients sensitive to drug side effects, including those with chronic underlying conditions. Overall, this study demonstrates that tail vein injection of the Lipo@miR-185-5p inhibitor, combined with the cardiac-targeting peptide APWHLSSQYSRT, enables effective targeting of heart tissue, significantly improves cardiac function, and inhibits myocardial fibrosis in a doxorubicin-induced dilated cardiomyopathy mouse model. This provides a novel approach and strategy for miRNA-based therapies in cardiovascular disease, aligning with emerging trends in precision medicine, where targeted delivery systems are increasingly recognized as essential for improving therapeutic outcomes and minimizing side effects.

These results further substantiate the effectiveness of miRNA delivery systems in cardiovascular disease models, and the use of heart-targeting peptides offers a promising strategy to optimize therapeutic efficacy. Compared to traditional

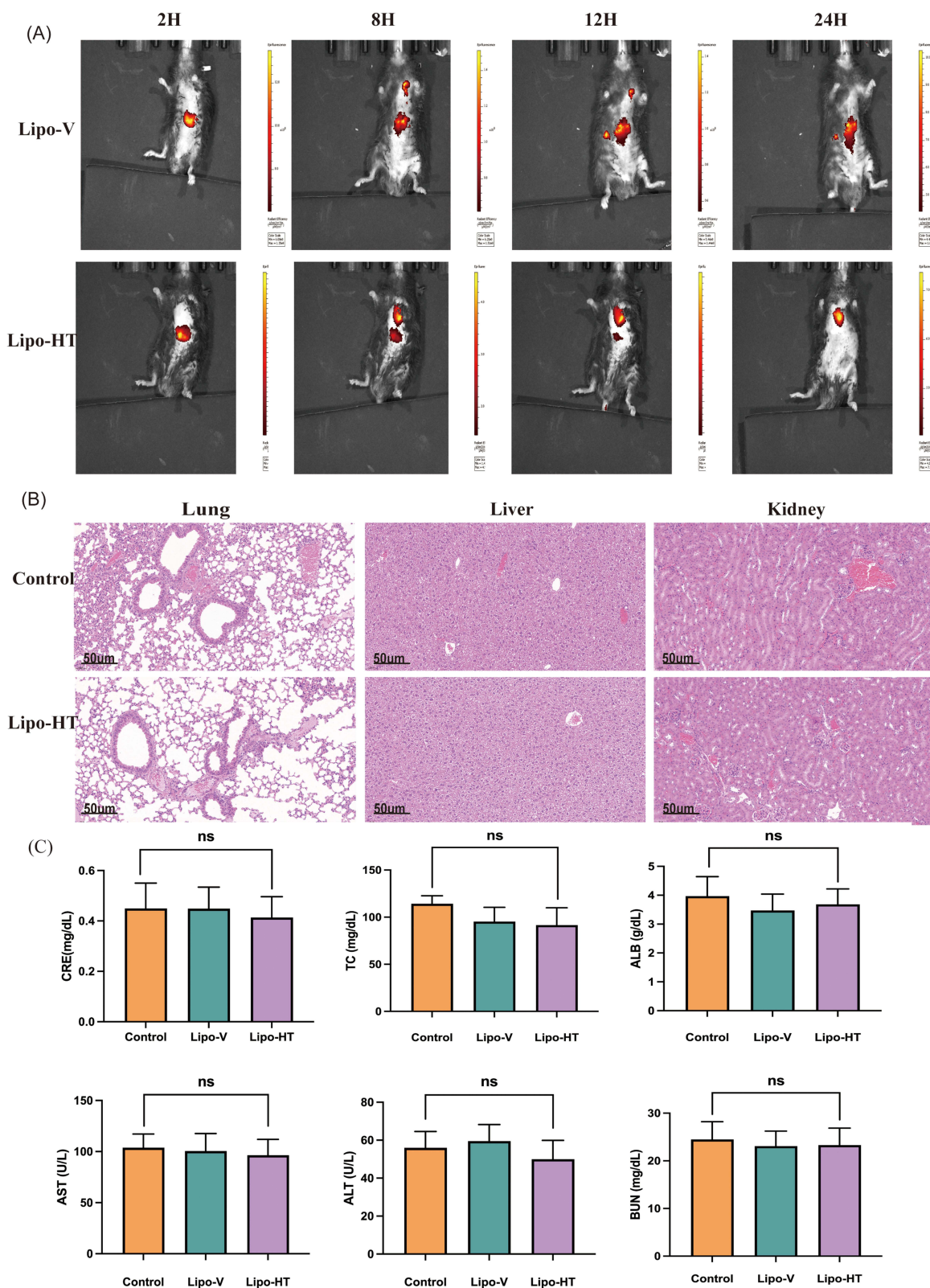


Figure 2 Biodistribution and biosafety of Lipo@miR-185-5p inhibitor: **(A)** Fluorescence imaging of Lipo-V and Lipo-HT biodistribution in mouse at 2, 8, 12, and 24 hours post-injection. Lipo-HT demonstrated significantly enhanced accumulation in cardiac tissue compared to Lipo-V over time. **(B)** In vivo biosafety evaluation of the liposome. Representative H&E staining images of main organs (lung, liver, and kidney) (scale bar = 50 μ m). **(C)** Serum biochemical parameters (CRE, TC, ALB, AST, ALT, BUN) in each group. Data are presented as mean \pm SD (n = 6 per group); ns = not significant.

approaches, this targeted miRNA delivery system could pave the way for more precise and effective treatments for heart diseases, potentially transforming therapeutic interventions in the field of cardiovascular medicine.³²

Therapeutic Efficacy of Lipo@miR-185-5p Inhibitor with Targeting Peptide in DCM Mouse Model

In this study, tail vein injection of Lipo@miR-185-5p inhibitor showed significant therapeutic effects in a DOX-induced mouse model of dilated cardiomyopathy (DCM). Mice were randomly divided into four groups. Echocardiographic analysis demonstrated a significant decline in cardiac function in the DOX group, with a marked reduction in left ventricular ejection fraction (EF) and fractional shortening (FS), confirming severe cardiac dysfunction (Figure 3A). In the DOX group, EF decreased significantly from $67.8\% \pm 3.4\%$ in the control group to $35.6\% \pm 4.2\%$ ($n=10$, $P < 0.01$), while FS dropped from $38.5\% \pm 3.2\%$ in the control group to $15.8\% \pm 2.6\%$ ($P < 0.01$) (Figure 3B). Treatment with Lipo@miR-185-5p inhibitor significantly restored cardiac function, with EF improving to $58.3\% \pm 3.1\%$ and FS recovering to $41.2\% \pm 3.9\%$ ($n=10$, both $P < 0.01$ compared to the DOX group). In contrast, the empty liposome group (Lipo) showed minimal improvement in EF and FS, highlighting the therapeutic specificity of the miRNA-encapsulated targeted liposomes. The DOX group demonstrated a significant reduction in Cardiac output (CO), decreasing from 12.5 ± 1.3 mL/min in the control group to 6.2 ± 0.9 mL/min ($P < 0.01$). Treatment with Lipo@miR-185-5p inhibitor resulted in a substantial enhancement of CO, reaching 10.8 ± 1.1 mL/min ($P < 0.01$), whereas the empty liposome group exhibited only a marginal effect (7.3 ± 1.2 mL/min) (Figure 3B). Heart rate (HR) was also significantly elevated in the DOX group, increasing from 560 ± 32 bpm in the control group to 735 ± 45 bpm ($P < 0.05$), indicative of compensatory tachycardia due to impaired cardiac function. Treatment with Lipo@miR-185-5p inhibitor resulted in a normalization of HR to 588 ± 40 bpm compared to the DOX group ($P < 0.05$), while the Lipo group exhibited limited effect, maintaining an elevated HR of 700 ± 38 bpm (Figure 3B).

Furthermore, the DOX group exhibited increased left ventricular end-diastolic diameter (LVEDD) and left ventricular end-systolic diameter (LVESD), indicative of severe ventricular remodeling. Both parameters were significantly reduced in the Lipo@miR-185-5p group, demonstrating improved ventricular structure and function. These results strongly indicate that Lipo@miR-185-5p inhibitor significantly improves cardiac function and mitigates ventricular remodeling in DCM.

Serum biomarkers were also assessed. Levels of cTnI, CK-MB, and NT-proBNP were significantly elevated in the DOX group, while treatment with Lipo@miR-185-5p inhibitor effectively reduced these markers (Figure S2), indicating decreased myocardial injuries.

Histological staining (HE) revealed severe myocardial damage in the DOX group, including pronounced myocardial disarray, necrosis, and interstitial inflammatory infiltration (Figure 3C). In contrast, the Lipo@miR-185-5p group exhibited a relatively intact myocardial structure, with orderly cell arrangement and notably fewer necrotic cells, demonstrating a clear protective effect. Furthermore, Masson staining revealed a substantial increase in myocardial fibrosis in the DOX group, indicative of extensive fibrotic remodeling (Figure 3D). Treatment with Lipo@miR-185-5p inhibitor led to a substantial reduction in fibrosis, further supporting its efficacy in alleviating DOX-induced myocardial injury and remodeling.

The results of this study demonstrate that Lipo@miR-185-5p inhibitor significantly improved cardiac function, reduced myocardial fibrosis, and decreased apoptosis in DOX-induced DCM mice.

To enhance cardiac-specific accumulation, we utilized the heart-targeting peptide APWHLSSQYSRT to functionalize liposomes. Previous studies have demonstrated the feasibility of such targeted delivery systems.^{33,34} Our findings demonstrate that the Lipo@miR-185-5p group showed significantly reduced myocardial fibrosis and apoptosis, indicating that the liposomal delivery system, enhanced by the targeting peptide, achieved specific accumulation in the heart, thus improving therapeutic outcomes.

In recent years, the use of heart-targeting peptides has gained increasing attention in the field of cardiovascular therapeutics.³⁵ Research by Cheng et al³⁶ demonstrated that targeting peptides can selectively accumulate drugs in heart tissue by binding to cardiac-specific receptors, thereby improving therapeutic efficacy and reducing toxicity in other organs. This aligns with our findings, where liposomes in the Lipo@miR-185-5p group accumulated significantly more in the heart compared to the empty liposome group, indicating that the heart-targeting peptide successfully enhanced the

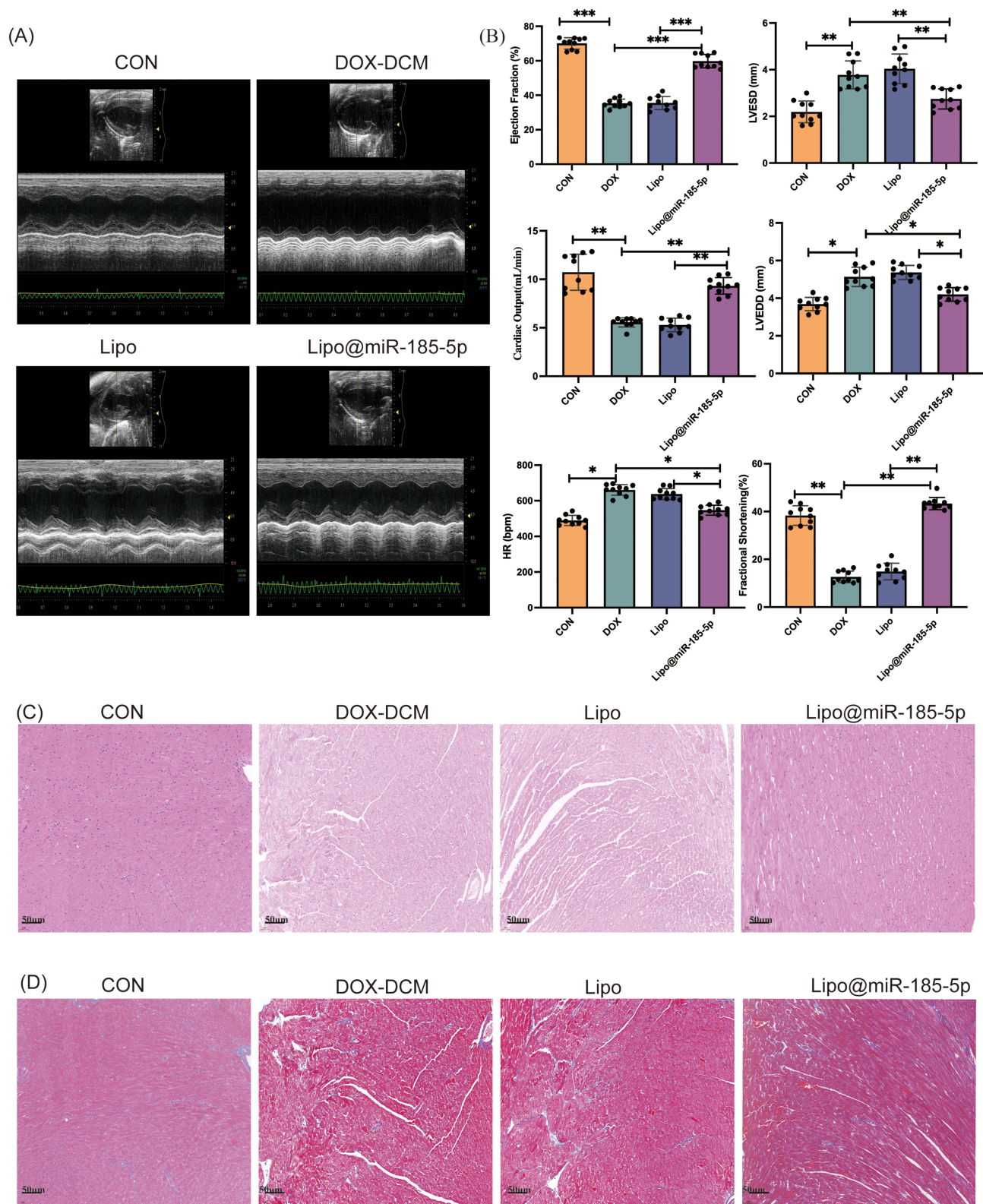


Figure 3 Cardiac function, myocardial integrity, and fibrosis assessment in a DOX-induced DCM mouse model treated with Lipo@miR-185-5p inhibitor. **(A)** Representative echocardiography images from each group, including Control (CON), DOX-DCM, empty liposome (Lipo), and Lipo@miR-185-5p groups. **(B)** Quantitative analysis of cardiac function parameters: ejection fraction (EF), fractional shortening (FS), left ventricular end-systolic diameter (LVESD), left ventricular end-diastolic diameter (LVEDD), cardiac output (CO), and heart rate (HR). Data are presented as mean ± SD (n=10). P < 0.05 *, P < 0.01 **, and P < 0.001 ***. **(C)** HE staining of myocardial tissues. Scale bar: 50 μm. **(D)** Masson staining of myocardial tissues. Scale bar: 50 μm.

liposomes' targeting capability. These results are consistent with other studies that report similar benefits when utilizing organ-specific peptides for targeted drug delivery, highlighting the potential of this approach to optimize treatment efficacy while minimizing side effects.³⁷

Furthermore, serum biochemical analysis showed no significant toxicity to liver and kidney function in the Lipo@miR-185-5p inhibitor group, further confirming the safety of this system. This finding is particularly important given the potential for systemic toxicity associated with conventional treatments, and it underscores the suitability of this formulation for patients with pre-existing conditions who may be more vulnerable to drug-induced toxicity. The lack of hepatotoxicity and nephrotoxicity in our study aligns with previous research indicating that lipid-based nanoparticles generally exhibit low toxicity profiles, supporting their use as safe and effective carriers for targeted therapies.³⁸

In summary, Lipo@miR-185-5p inhibitor with targeting peptide exhibits potent cardioprotective effects and offers a promising platform for miRNA-based therapy in DCM. Future work should focus on optimizing the liposomal formulation and evaluating other organ-targeting peptides to extend this strategy's applicability.

Lipo@miR-185-5p Inhibitor Effectively Ameliorates DCM by Reducing Apoptosis and Copper-Induced Cell Death

In this study, the Lipo@miR-185-5p inhibitor, delivered via a heart-targeted liposomal system, exhibited significant therapeutic effects in an *in vitro* model of dilated cardiomyopathy (DCM). Human iPSC-derived cardiomyocytes (hiPSC-CMs) were successfully generated and used as the cellular model for this study, with successful differentiation confirmed by the observation of spontaneous beating, a characteristic feature of cardiomyocytes (Figure S3).³⁹ Prior to the intervention, the optimal concentration of Lipo@miR-185-5p inhibitor was determined using a CCK8 assay, with the results shown in Figure S4. In iPSC-derived cardiomyocyte models, we assessed the expression of apoptotic and cuproptosis markers by Western blotting (Figure 4A and B). Compared to the control group (CON), the DOX-induced group (DOX) exhibited a pronounced apoptotic and cuproptosis phenotype, evidenced by significant upregulation of pro-apoptotic proteins, including BAX and Cleaved-Caspase3 (CC3) (both $P < 0.01$), along with a marked downregulation of the anti-apoptotic protein BCL-2 ($P < 0.01$). Furthermore, the expression of cuproptosis-related proteins, including DLAT, DLST, and FDX1, was also significantly increased (all $P < 0.01$), suggesting that DOX-induced cellular damage may encompass both apoptosis and cuproptosis. Treatment with the Lipo@miR-185-5p inhibitor led to a significant reduction in the expression of BAX and CC3, while restoring BCL-2 levels ($P < 0.01$). The expression of cuproptosis markers DLAT, DLST, and FDX1 was also markedly diminished after treatment (all $P < 0.01$), indicating that the Lipo@miR-185-5p inhibitor effectively suppressed both DOX-induced apoptosis and cuproptosis.

To further validate these findings, a DCM *in vitro* model was established using H9C2 cells ($n = 3$ per group for each assay). Cell apoptosis, DNA damage, and oxidative stress were then assessed via immunofluorescence staining. TUNEL staining revealed a significant increase in TUNEL-positive cells in the DOX-induced group (DOX), indicating substantial apoptosis induced by DOX ($P < 0.01$, Figure 4C). However, in the Lipo@miR-185-5p treatment group, the number of TUNEL-positive cells was significantly reduced compared to the DOX group ($P < 0.01$), confirming the anti-apoptotic effect of Lipo@miR-185-5p. Concurrently, γ H2AX staining was used to detect DNA double-strand breaks. In the DOX group, γ H2AX-positive signals were markedly enhanced, indicating extensive DNA damage induced by DOX. In contrast, Lipo@miR-185-5p treatment significantly reduced γ H2AX-positive DNA damage ($P < 0.01$, Figure 4D). Additionally, oxidative stress levels were assessed using ROS probes, and cells in the DOX group displayed a significant increase in ROS levels, suggesting that oxidative stress plays a crucial role in DOX-induced cardiomyocyte damage. In the Lipo@miR-185-5p treatment group, ROS levels were significantly decreased compared to the DOX group ($P < 0.01$), indicating that Lipo@miR-185-5p inhibitor also effectively mitigated oxidative stress (Figure 4E).

Lipo@miR-185-5p inhibitor demonstrates significant therapeutic effects in doxorubicin (DOX)-induced cardiomyocyte injury by reducing both apoptosis and cuproptosis, highlighting its unique potential in cardiovascular diseases. The regulatory role of miRNAs in various cellular processes has been widely studied, particularly in cardiovascular diseases, where miRNAs act as key molecular regulators, modulating cellular signaling pathways that can have protective or pathogenic effects.⁸ In this study, the targeted inhibition of miR-185-5p plays a central role in regulating both apoptosis

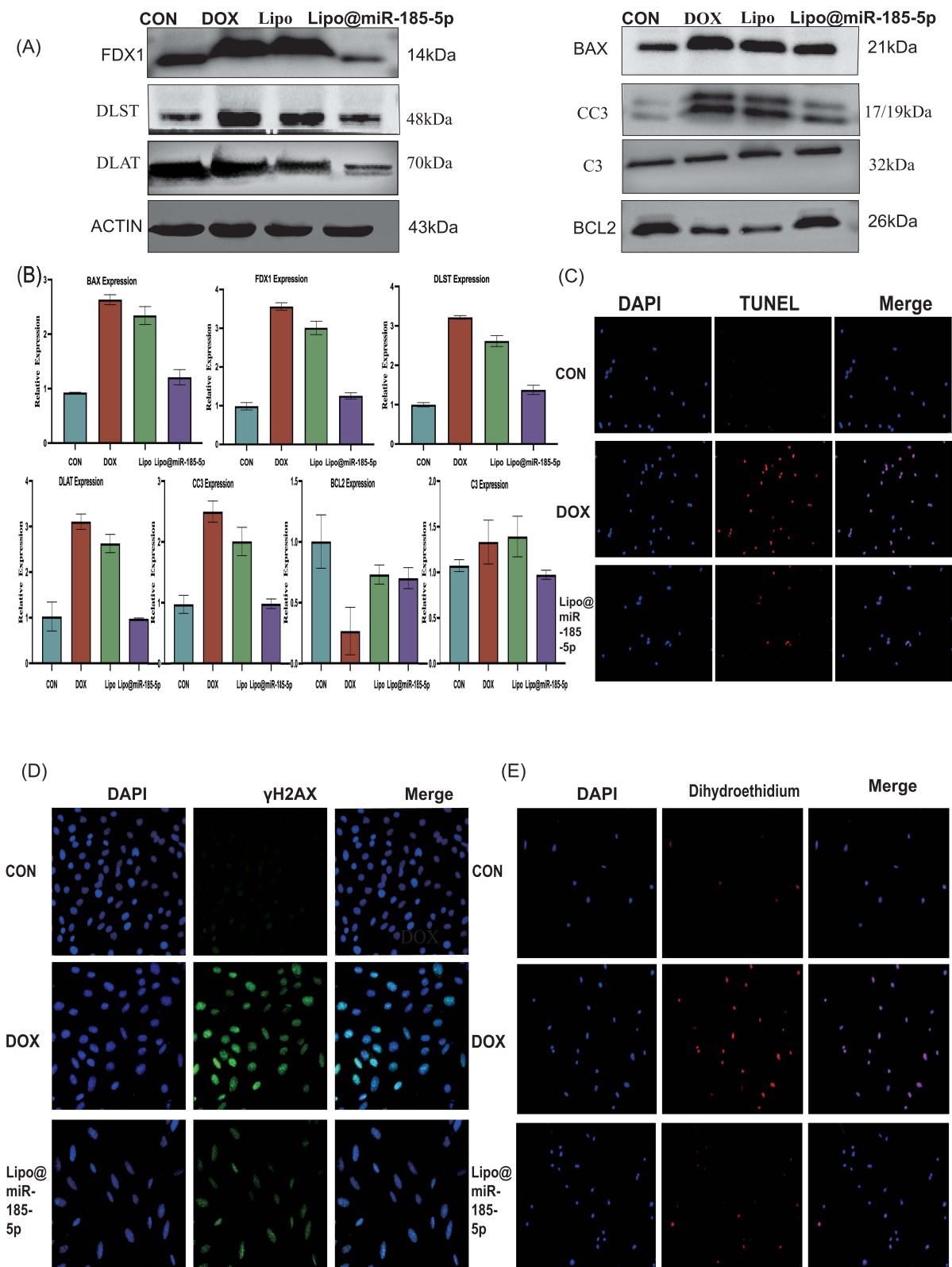


Figure 4 Lipo@miR-185-5p inhibitor suppressed DOX-induced apoptosis, cuproptosis, and oxidative stress in cardiomyocyte models. **(A)** Western blot analysis showed reduced pro-apoptotic (BAX, CC3) and cuproptosis (DLAT, DLST, FDX1) markers and increased anti-apoptotic (BCL-2) protein expression after treatment. **(B)** Quantitative analysis of Western blot results. **(C)** TUNEL staining revealed decreased apoptosis in the Lipo@miR-185-5p group. **(D)** γH2AX staining indicated reduced DNA damage. **(E)** ROS staining demonstrated alleviated oxidative stress with Lipo@miR-185-5p treatment. Data are presented as mean ± SD (n = 3 per group).

and cuproptosis. Measurement of myocardial copper levels revealed that DOX treatment significantly elevated cardiac Cu^{2+} concentrations compared to controls (25.04 ± 1.73 $\mu\text{mol/L}$ vs 5.12 ± 0.89 $\mu\text{mol/L}$, $P < 0.01$). Administration of Lipo@miR-185-5p inhibitor markedly reduced Cu^{2+} levels (10.06 ± 1.48 $\mu\text{mol/L}$, $P < 0.01$), whereas treatment with empty liposomes resulted in only a slight decrease (22.95 ± 1.95 $\mu\text{mol/L}$) (Figure S5). These findings provide direct evidence supporting copper dysregulation in DOX-induced DCM and demonstrate the therapeutic efficacy of Lipo@miR-185-5p inhibitor in restoring copper homeostasis. Cuproptosis, a novel form of programmed cell death, primarily induces cell death through mechanisms such as the inactivation of iron-sulfur cluster proteins, accumulation of lipid peroxides, and disruption of energy metabolism.²⁰ During the pathological progression of DCM, cuproptosis may further exacerbate myocardial apoptosis and fibrosis. Therefore, the specific inhibition of cuproptosis presents a promising therapeutic target for cardiovascular diseases.

Our results indicate that Lipo@miR-185-5p inhibitor not only alleviates cell death by inhibiting apoptosis pathways, but also prevents cuproptosis by suppressing the expression of key proteins associated with cuproptosis. This multi-target regulatory mechanism provides broad therapeutic potential, making miRNA inhibitors more versatile compared to traditional drugs.⁴⁰ Moreover, the liposomal delivery system, in combination with the cardiac-targeting peptide APWHLSSQYSRT, facilitates highly efficient miRNA delivery to cardiac tissue. Liposomes offer high biocompatibility and drug-loading capacity, but conventional formulations often lack targeting specificity, leading to off-target distribution and reduced therapeutic efficacy.⁴¹ In this study, by introducing a cardiac-specific targeting peptide, Lipo@miR-185-5p inhibitor significantly enhanced cardiac accumulation and reduced drug accumulation in non-target organs. This targeted delivery strategy overcomes the limitations of conventional gene therapies, improving therapeutic efficacy while reducing potential systemic toxicity. Our experimental results show that Lipo@miR-185-5p inhibitor accumulated significantly more in cardiac tissue compared to the empty liposome group. Furthermore, serum biochemical markers indicated no significant adverse effects on liver and kidney function, thus confirming the high targeting efficiency and safety of this system.

The multi-target regulatory mechanism of Lipo@miR-185-5p inhibitor provides significant advantages in the treatment of cardiovascular diseases. In the DCM model, cardiomyocytes undergo not only apoptosis but also oxidative stress, DNA damage, and cuproptosis, among other pathological processes. These processes interact, accelerating myocardial damage progression. By regulating miR-185-5p inhibition, we are able to simultaneously inhibit multiple pathological processes, thereby protecting cardiomyocytes at various levels. Immunofluorescence results from this study show that Lipo@miR-185-5p inhibitor significantly reduces cell apoptosis (TUNEL-positive cells), DNA damage (γH2AX -positive markers), and oxidative stress (ROS levels). These findings indicate that this therapy not only prevents cardiomyocyte apoptosis but also effectively reduces cellular damage and alleviates oxidative stress.

MiR-185-5p used in this study was extracted from plasma-derived exosomes, a source we chose to build upon our previous research.¹⁰ Exosomes are known to play a crucial role in intercellular communication and have demonstrated potential in the targeted delivery of miRNAs. The combination of exosome-derived miR-185-5p with liposomal carriers enhances both the stability and bioavailability of the miRNA, offering a more efficient and safer therapeutic option. This exosome-liposome hybrid delivery system exploits the unique properties of both platforms, ensuring targeted, sustained release of the therapeutic miRNA to the heart.⁴² This study validates the multi-layered protective effects of Lipo@miR-185-5p inhibitor in the doxorubicin-induced dilated cardiomyopathy model, significantly improving myocardial cell injury by reducing apoptosis, inhibiting cuproptosis, and alleviating oxidative stress. In addition, the employment of a liposomal delivery system in conjunction with a heart-targeting peptide not only enhances the specificity of treatment but also mitigates systemic toxicity, underscoring its substantial potential for clinical application. The overall animal experimental workflow is illustrated in Supplementary Figure S6. Subsequent studies may further refine the liposomal composition and targeting properties to enhance clinical efficacy and investigate its potential application in other cardiovascular diseases.

Conclusion

In summary, this study presents a novel therapeutic strategy for doxorubicin-induced dilated cardiomyopathy (DCM) using a dual-targeting nanocarrier system to deliver a miR-185-5p inhibitor with enhanced cardiac specificity. By simultaneously modulating apoptosis and cuproptosis—two key pathological mechanisms in DCM—the treatment markedly attenuates myocardial injury and preserves cardiac function. The integration of a cardiac-targeting peptide

significantly improves tissue selectivity, addressing the off-target limitations of conventional liposomal systems. Notably, the miRNA inhibitor was derived from plasma exosomes, and its encapsulation within engineered liposomes combines the intrinsic biological targeting capacity of exosomes with the customizable delivery efficiency of synthetic nanocarriers. This hybrid platform enhances stability, bioavailability, and cardiac-specific accumulation. Altogether, this bioengineered delivery system demonstrates clear advantages over previously reported approaches by integrating pathological relevance, high encapsulation efficiency, and organ-targeted precision. These findings support the therapeutic potential of Lipo@miR-185-5p as a candidate for RNA-based intervention in DCM and provide a promising foundation.

Abbreviations

DCM, Dilated cardiomyopathy; miRNA, MicroRNA; DCM-HF, Dilated cardiomyopathy combined with heart failure; Lipo@miR-185-5p inhibitor, miRNA-185-5p inhibitors within liposomes; LV, left ventricular; ACE, angiotensin-converting enzyme; ARNIs, angiotensin receptor-neprilysin inhibitors.

SGLT2, sodium-glucose cotransporter-2; FDA, Food and Drug Administration; CCK-8, cell counting kit-8; TC, total cholesterol; ALT, alanine aminotransferase; AST, aspartate aminotransferase; ALB, albumin; BUN, blood urea nitrogen; CRE, creatinine; TEM, transmission electron microscopy; FBS, fetal bovine serum; Dox, Doxorubicin; DLS, dynamic light scattering; Lipo-V, non-targeted liposome group; Lipo-HT, heart-targeted peptide-modified liposome group.

Data Sharing Statement

The data presented in this study are available on request from the Professor Yafeng Zhou.

Acknowledgments

This work was supported by grants from National Natural Science Foundation of China (81873486), the Science and Technology Development Program of Jiangsu Province-Clinical Frontier Technology (BE2022754), Clinical Medicine Expert Team (Class A) of Jinji Lake Health Talents Program of Suzhou Industrial Park (SZYQTD202102), Suzhou Key Discipline for Medicine (SZXK202129), Demonstration of Scientific and Technological Innovation Project (SKY2021002), Suzhou Dedicated Project on Diagnosis and Treatment Technology of Major Diseases (LCZX202132), Research on Collaborative Innovation of medical engineering combination (SZM2021014), Research on Collaborative Innovation of medical engineering combination (SZM2022003), Suzhou Key Laboratory of Diagnosis and Treatment of Panvascular Diseases (SZS2023021). Postgraduate Research & Practice Innovation Program of Jiangsu Province (SJCX25_1796). National Natural Science Foundation of China (Nos. 82222007, 82170281, U2004203, 81800267), the Henan Thousand Talents Program (No. ZYQR201912131), the Excellent Youth Science Foundation of Henan Province (No. 202300410362), Henan Province Medical Science and Technology Key Joint Project (SBGJ202101012), Central Plains Youth Top Talent, Advanced funds (No. 2021-CCA-ACCESS-125), Funding for Scientific Research and Innovation Team of The First Affiliated Hospital of Zhengzhou University (QNCXTD2023001,ZYCXTD2023008).

Disclosure

The authors report no conflicts of interest in this work.

References

- Heymans S, Lakdawala NK, Tschöpe C, Klingel K. Dilated cardiomyopathy: causes, mechanisms, and current and future treatment approaches. *Lancet*. 2023;402(10406):998–1011. doi:10.1016/s0140-6736(23)01241-2
- Japp AG, Gulati A, Cook SA, Cowie MR, Prasad SK. The Diagnosis and Evaluation of Dilated Cardiomyopathy. *J Am Coll Cardiol*. 2016;67(25):2996–3010. doi:10.1016/j.jacc.2016.03.590
- Weintraub RG, Semsarian C, Macdonald P. Dilated cardiomyopathy. *Lancet*. 2017;390(10092):400–414. doi:10.1016/s0140-6736(16)31713-5
- Merlo M, Cannatà A, Gobbo M, Stolfo D, Elliott PM, Sinagra G. Evolving concepts in dilated cardiomyopathy. *Eur J Heart Fail*. 2018;20(2):228–239. doi:10.1002/ehf.1103
- McNally EM, Mestroni L. Dilated Cardiomyopathy. *Circ Res*. 2017;121(7):731–748. doi:10.1161/circresaha.116.309396
- Elliott P. CARDIOMYOPATHY: diagnosis and management of dilated cardiomyopathy. *Heart*. 2000;84(1):106–112. doi:10.1136/heart.84.1.106
- Sorella A, Galanti K, Iezzi L, et al. Diagnosis and management of dilated cardiomyopathy: a systematic review of clinical practice guidelines and recommendations. *Eur Heart J Qual Care Clin Outcomes*. 2024. doi:10.1093/ehjqcco/qcae109

8. Diener C, Keller A, Meese E. Emerging concepts of miRNA therapeutics: from cells to clinic. *Trends Genet.* 2022;38(6):613–626. doi:10.1016/j.tig.2022.02.006
9. Eldemire R, Mestroni L, Taylor MRG. Genetics of Dilated Cardiomyopathy. *Annu Rev Med.* 2024;75(1):417–426. doi:10.1146/annurev-med-052422-020535
10. Zhang L, Zhang G, Lu Y, et al. Differential expression profiles of plasma exosomal microRNAs in dilated cardiomyopathy with chronic heart failure. *J Cell Mol Med.* 2023;27(14):1988–2003. doi:10.1111/jcmm.17789
11. Lin R, Rahtu-Korpela L, Szabo Z, et al. MiR-185-5p regulates the development of myocardial fibrosis. *J Mol Cell Cardiol.* 2022;165:130–140. doi:10.1016/j.yjmcc.2021.12.011
12. Wang T, Li N, Yuan L, et al. MALAT1/miR-185-5p mediated high glucose-induced oxidative stress, mitochondrial injury and cardiomyocyte apoptosis via the RhoA/ROCK pathway. *J Cell Mol Med.* 2023;27(17):2495–2506. doi:10.1111/jcmm.17835
13. Cheng Z, Li M, Dey R, Chen Y. Nanomaterials for cancer therapy: current progress and perspectives. *J Hematol Oncol.* 2021;14(1):85. doi:10.1186/s13045-021-01096-0
14. Zylberberg C, Matosevic S. Pharmaceutical liposomal drug delivery: a review of new delivery systems and a look at the regulatory landscape. *Drug Deliv.* 2016;23(9):3319–3329. doi:10.1080/10717544.2016.1177136
15. Large DE, Abdelmessih RG, Fink EA, Auguste DT. Liposome composition in drug delivery design, synthesis, characterization, and clinical application. *Adv Drug Deliv Rev.* 2021;176:113851. doi:10.1016/j.addr.2021.113851
16. Wang R, Wang X, Zhao H, et al. Targeted delivery of hybrid nanovesicles for enhanced brain penetration to achieve synergistic therapy of glioma. *J Control Release.* 2024;365:331–347. doi:10.1016/j.jconrel.2023.11.033
17. d'Avanzo N, Torrieri G, Figueiredo P, et al. LinTT1 peptide-functionalized liposomes for targeted breast cancer therapy. *Int J Pharm.* 2021;597:120346. doi:10.1016/j.ijpharm.2021.120346
18. Tan H, Song Y, Chen J, et al. Platelet-Like Fusogenic Liposome-Mediated Targeting Delivery of miR-21 Improves Myocardial Remodeling by Reprogramming Macrophages Post Myocardial Ischemia-Reperfusion Injury. *Adv Sci.* 2021;8(15):e2100787. doi:10.1002/advs.202100787
19. Yin H, Guo X, Chen Y, et al. AB2 deficiency induces dilated cardiomyopathy by promoting RIPK1-dependent apoptosis and necroptosis. *J Clin Invest.* 2022;132(4). doi:10.1172/jci152297
20. Yang L, Yang P, Lip GYH, Ren J. Copper homeostasis and cuproptosis in cardiovascular disease therapeutics. *Trends Pharmacol Sci.* 2023;44(9):573–585. doi:10.1016/j.tips.2023.07.004
21. Huo S, Wang Q, Shi W, et al. ATF3/SPI1/SLC31A1 Signaling Promotes Cuproptosis Induced by Advanced Glycosylation End Products in Diabetic Myocardial Injury. *Int J Mol Sci.* 2023;24(2). doi:10.3390/ijms24021667
22. Sheng SY, Li JM, Hu XY, Wang Y. Regulated cell death pathways in cardiomyopathy. *Acta Pharmacol Sin.* 2023;44(8):1521–1535. doi:10.1038/s41401-023-01068-9
23. Bhavsar D, Subramanian K, Sethuraman S, Krishnan UM. EpCAM-targeted liposomal si-RNA delivery for treatment of epithelial cancer. *Drug Deliv.* 2016;23(4):1101–1114. doi:10.3109/10717544.2014.973082
24. Li L, He D, Guo Q, et al. Exosome-liposome hybrid nanoparticle codelivery of TP and miR497 conspicuously overcomes chemoresistant ovarian cancer. *J Nanobiotechnology.* 2022;20(1):50. doi:10.1186/s12951-022-01264-5
25. Sun F, Chen H, Dai X, et al. Liposome-lentivirus for miRNA therapy with molecular mechanism study. *J Nanobiotechnology.* 2024;22(1):329. doi:10.1186/s12951-024-02534-0
26. Feng X, Wen Z, Zhu X, Yan X, Duan Y, Huang Y. Anti-HER2 immunoliposomes: antitumor efficacy attributable to targeted delivery of anthraquinone-fused enediynes. *Adv Sci.* 2024;11(17):e2307865. doi:10.1002/advs.202307865
27. Segvich SJ, Smith HC, Kohn DH. The adsorption of preferential binding peptides to apatite-based materials. *Biomaterials.* 2009;30(7):1287–1298. doi:10.1016/j.biomaterials.2008.11.008
28. Li M, Tang X, Liu X, et al. Targeted miR-21 loaded liposomes for acute myocardial infarction. *J Mater Chem B.* 2020;8(45):10384–10391. doi:10.1039/d0tb01821j
29. Chen X, Meng F, Xu Y, Li T, Chen X, Wang H. Chemically programmed STING-activating nano-liposomal vesicles improve anticancer immunity. *Nat Commun.* 2023;14(1):4584. doi:10.1038/s41467-023-40312-y
30. Wang S, Zhang Y, Zhong Y, et al. Accelerating diabetic wound healing by ROS-scavenging lipid nanoparticle–mRNA formulation. *Proc Natl Acad Sci USA.* 2024;121(22):e2322935121. doi:10.1073/pnas.2322935121
31. Weng H, Zou W, Tian F, et al. Inhalable cardiac targeting peptide modified nanomedicine prevents pressure overload heart failure in male mice. *Nat Commun.* 2024;15(1):6058. doi:10.1038/s41467-024-50312-1
32. Zhang X, Rotllan N, Canfrán-Duque A, et al. Targeted suppression of miRNA-33 using pHILIP improves atherosclerosis regression. *Circ Res.* 2022;131(1):77–90. doi:10.1161/circresaha.121.320296
33. Allen TM, Cullis PR. Liposomal drug delivery systems: from concept to clinical applications. *Adv Drug Deliv Rev.* 2013;65(1):36–48. doi:10.1016/j.addr.2012.09.037
34. Sun D, Tan S, Xiong Y, et al. MicroRNA biogenesis is enhanced by liposome-encapsulated pin1 inhibitor in hepatocellular carcinoma. *Theranostics.* 2019;9(16):4704–4716. doi:10.7150/thno.34588
35. Kang JY, Mun D, Chun Y, et al. Engineered small extracellular vesicle-mediated NOX4 siRNA delivery for targeted therapy of cardiac hypertrophy. *J Extracell Vesicles.* 2023;12(10):e12371. doi:10.1002/jev2.12371
36. Vandergriff A, Huang K, Shen D, et al. Targeting regenerative exosomes to myocardial infarction using cardiac homing peptide. *Theranostics.* 2018;8(7):1869–1878. doi:10.7150/thno.20524
37. Mousavizadeh A, Jabbari A, Akrami M, Bardania H. Cell targeting peptides as smart ligands for targeting of therapeutic or diagnostic agents: a systematic review. *Colloids Surf B Biointerfaces.* 2017;158:507–517. doi:10.1016/j.colsurfb.2017.07.012
38. Fu Q, Li G, Wang L, et al. Tumor supplying artery injection of Liposome@ sunitinib could effectively inhibit the progression of kidney tumor. *ACS Appl Mater Interfaces.* 2024. doi:10.1021/acsami.4c00729
39. Prondzynski M, Berkson P, Trembley MA, et al. Efficient and reproducible generation of human iPSC-derived cardiomyocytes and cardiac organoids in stirred suspension systems. *Nat Commun.* 2024;15(1):5929. doi:10.1038/s41467-024-50224-0
40. Su D, Chen Z, An X, et al. MicroRNA-195 liposomes for therapy of Alzheimer's disease. *J Control Release.* 2024;365:583–601. doi:10.1016/j.jconrel.2023.12.003

41. Zhang W, Gong C, Chen Z, Li M, Li Y, Gao J. Tumor microenvironment-activated cancer cell membrane-liposome hybrid nanoparticle-mediated synergistic metabolic therapy and chemotherapy for non-small cell lung cancer. *J Nanobiotechnology*. 2021;19(1):339. doi:10.1186/s12951-021-01085-y
42. Wu S, Yun J, Tang W, et al. Therapeutic m6A eraser ALKBH5 mRNA-loaded exosome–liposome hybrid nanoparticles inhibit progression of colorectal cancer in preclinical tumor models. *ACS Nano*. 2023;17(12):11838–11854. doi:10.1021/acsnano.3c03050

International Journal of Nanomedicine

Publish your work in this journal

The International Journal of Nanomedicine is an international, peer-reviewed journal focusing on the application of nanotechnology in diagnostics, therapeutics, and drug delivery systems throughout the biomedical field. This journal is indexed on PubMed Central, MedLine, CAS, SciSearch®, Current Contents®/Clinical Medicine, Journal Citation Reports/Science Edition, EMBase, Scopus and the Elsevier Bibliographic databases. The manuscript management system is completely online and includes a very quick and fair peer-review system, which is all easy to use. Visit <http://www.dovepress.com/testimonials.php> to read real quotes from published authors.

Submit your manuscript here: <https://www.dovepress.com/international-journal-of-nanomedicine-journal>

Dovepress
Taylor & Francis Group